Abstract

Purpose: To investigate the time-course of foveal development after birth in infants with albinism.

Design: Prospective, comparative cohort optical coherence tomography (OCT) study

Methods: 36 children with albinism were recruited. All participants were aged between 0 and 6 years and were seen at Leicester Royal Infirmary. A total of 181 mixed cross-sectional and longitudinal OCT examinations were obtained, which were analyzed for differences in retinal development in comparison to 297 cross-sectional control examinations.

Results: Normal retinal development involves migration of the inner retinal layers (IRLs) away from the fovea, migration of the cone photoreceptors into the fovea and elongation of the outer retinal layers (ORLs) over time. In contrast to controls where IRL migration from the fovea was almost completed at birth, a significant degree of IRL migration was taking place after birth in albinism, before arresting prematurely at 40 months postmenstrual age (PMA). This resulted in a significantly thicker central macular thickness in albinism (Δ=83.8±6.1, p<0.0001 at 69 months PMA). There was evidence of ongoing foveal ORL elongation in albinism, although reduced in amplitude compared to controls after 21 months PMA (Δ=-17.3±4.3, p<0.0001).

Conclusions: We have demonstrated evidence of ongoing retinal development in young children with albinism, albeit at a reduced rate and magnitude compared to controls. The presence of a period of retinal plasticity in early childhood raises the possibility that treatment modalities, which aim to improve retinal development, could potentially optimize visual function in albinism.

Retinal development in infants and young children with albinism: evidence for plasticity in early childhood.

Helena Lee [1], Ravi Purohit[1], Viral Sheth[1], Gail Maconachie[1], Zhanhan Tu[1], Mervyn G Thomas[1], Anastasia Pilat[1], Rebecca J McLean[1], Frank A Proudlock[1], and Irene Gottlob[1]

[1]The University of Leicester Ulverscroft Eye Unit, Robert Kilpatrick Clinical Sciences Building, PO Box 65, Leicester Royal Infirmary, Leicester, LE2 7LX, UK

Corresponding author: Dr Helena Lee
Clinical and Experimental Sciences,
Faculty of Medicine,
University of Southampton,
Mailpoint 806, Level D,
Southampton University Hospital,
Tremona Road,
Southampton,
SO16 6YD
Helena.Lee@soton.ac.uk
+447775363943

Supplemental Material available at AJO.com.

The following authors have updated affiliations: Helena Lee: Faculty of Medicine, University of Southampton, Ravi Purohit: Orthoptic Department, The Oxford Eye Hospital LG1, West Wing John Radcliffe Hospital Headley Way Headington Oxford OX3 9DU & Nuffield department of clinical neurosciences (NDCN), Level 6, West Wing, John Radcliffe Hospital, Oxford OX3 9DU: Viral Sheth & Gail Maconachie: Academic Unit of Ophthalmology and Orthoptics, University of Sheffield, Sheffield, S10 2TX, UK; Anastasia Pilat: East Sussex NHS Healthcare Trust, Kings Dr, Eastbourne BN21 2UD, Irene Gottlob: Department of Neurology, Cooper University Hospital, Cooper Neurological Institute, 2339 Route 70 West 4th Floor Cherry Hill, NJ, 08002 USA & Professor of Neurology, Cooper Medical School of Rowan University, Camden, NJ 08103 USA

Meeting Presentation: Association for Research in Vision and Ophthalmology (ARVO) meeting 2016, British Isles Paediatric, Ophthalmology & Strabismus Association (BIPOSA) meeting 2015

Short title: Retinal Development in Albinism

Key Words: Albinism, Retinal Development, Optical Coherence Tomography

Word Count: 3089

Table of Contents Statement

In this prospective, comparative cohort) study of *in vivo* retinal development in 36 children with albinism, evidence of ongoing retinal development in early childhood in albinism has been demonstrated using *in vivo* hand-held optical coherence tomography imaging. Potentially treatment during this critical period may improve retinal development and optimize visual function

Introduction

Albinism is a group of disorders of melanin biosynthesis that affects approximately 1 in 4000 people in the United Kingdom and are characterized by cutaneous and/or ocular hypo-pigmentation, nystagmus, strabismus, refractive errors, foveal hypoplasia and optic nerve misrouting.[1,2] It is hypothesized that normal foveal development is arrested in individuals with albinism resulting in foveal hypoplasia (persistence of the normally absent inner retinal layers (IRLs) at the fovea).[3,4] However, we have recently shown that normal retinal development continues until early adolescence and it remains unclear if postnatal development is arrested or continues in an altered spatial and temporal pattern in infants and young children with albinism.[5]

Normal pigmentation and development of the eye are dependent upon the presence of a functioning tyrosinase (TH) enzyme[6], which catalyzes the conversion of tyrosine to dihydroxyphenylalanine (DOPA), phaeomelanin, eumelanin and dopamine (DA).[7,8] This pathway is disrupted in albinism, with a consequential deficiency of several key molecules essential for normal retinal development. As a result, retinal development in albinism is altered in several ways including an abnormal division pattern of the retinal progenitors from the early stages[9-12], abnormal decussation of ganglion cell axons[10,11] with chiasmal misrouting[13], an abnormal pattern of apoptosis and mitosis during post-natal development[10,14,15] and a reduction in the number of photoreceptors. [9,11,16] Most of these studies are based on animal or *in vitro* models with very little work performed on *in vivo* retinal development in humans affected by albinism. The recent development of hand-held spectral domain optical coherence tomography (HH-SDOCT) technology which can reliably obtain high resolution cross-sectional retinal imaging *in vivo* in infants and young children provides the ability to remedy this limitation.[17,18]

Several components of the melanin/DA synthesis pathway are being targeted as potential treatment options in oculocutaneous albinism (OCA).[19-22] Postnatal nonsense

mutation suppression treatment strategies have also demonstrated potential in *PAX6* mutations, another condition associated with foveal hypoplasia.[23,24] With these therapies potentially becoming available, it is important to develop a detailed understanding of *in vivo* human retinal development in albinism so that further therapeutic targets can be identified, the timing of treatment can be optimized and treatment outcomes can be objectively assessed. We therefore performed a longitudinal HH-SDOCT study of *in vivo* foveal development, in a cohort of 36 children aged between birth and 6 years of age, with a diagnosis of albinism. Our aim was to investigate whether foveal hypoplasia in albinism is associated with arrested retinal development after birth or if further retinal development occurs after birth reflecting neuronal plasticity.

Methods

Study design & Participants

This was a prospective, comparative cohort OCT study of *in vivo* retinal development in albinism. Informed consent was obtained from all parents/guardians of patients and control subjects participating in this study. The study adhered to the tenets of the Declaration of Helsinki, and was prospectively approved by the NRES Committee East Midlands – Nottingham 2; REC reference 12/EM/0261: Characterisation of normal and abnormal ocular development using ultra-high resolution optical coherence tomography (UHR-SD OCT). The cohort for this study included 43 children with a confirmed clinical diagnosis of albinism (Supplementary Table 1) and 148 age and race-matched controls. Albinism was diagnosed based on previously established diagnostic criteria[25] as follows:

- 3 major criteria or
- 2 major and 2 minor criteria for the diagnosis of albinism or
- In the presence of a molecular diagnosis, 1 major criterion or 2 minor criteria for the diagnosis of albinism was sufficient.

Major criteria

- Foveal hypoplasia grade 2 or more
- Optic nerve misrouting on visual evoked potential (VEP) testing
- Ocular hypopigmentation, either Iris transillumination defects or fundus hypopigmentation grade 2 or more

Minor criteria

- Infantile nystagmus
- Cutaneous hypopigmentation
- Grade 1 fundus hypopigmentation

Molecular diagnosis

- A genotype consisting of 1 previously published pathogenic variant in a known OCA gene or 1 novel variant deemed 'highly likely' to be pathogenic & either
    - A 2nd known or novel 'highly likely' pathogenic variant in the same gene or
    - A 2nd common variant in the same gene, known to be associated with an albino phenotype

A total of 181 mixed cross-sectional and longitudinal HH-SDOCT examinations were obtained, which included 93 (51.3%) and 88 (48.6%) tomograms obtained from the right and left eyes respectively, in the albinism group. These were compared to 297 cross-sectional control examinations, which included 151 (50.8%) and 146 (49.2%) tomograms obtained from the right and left eyes respectively.

In order to select the appropriate control examinations for comparison from our previously published normative database[5], the albinism scans were divided into 14 age groups as follows: less than 40 weeks gestational age (GA), 41 to 46 weeks GA, 47 to 52 weeks GA, 2 to 5 months, 6 to 8 months, 9 to 11 months, 12 to 17 months, 18 to 23 months, 24 to 29 months, 30 to 35 months, 3 years, 4 years, 5 years and 6 years. They were also divided by race as follows: Caucasian, Asian or Afro-Caribbean. Only the control OCT examinations that matched both the age group and race of each albinism OCT examination obtained were included for comparison. The mean postnatal age at the time of examination was 37.8 months (range 0.9 - 83.6) for the albinism group and 37.7 months (range 0 - 83.3) for the control group.

All participants underwent a full orthoptic and ophthalmologic examination, which included slit-lamp examination (where possible), fundus examination and measurement of visual acuity (VA). VA was assessed in younger infants and children by preferential looking using Teller acuity cards. In cooperative children, Teller acuity cards and/or logMAR crowded

optotypes (Glasgow Acuity Cards) were used. The clinical characteristics of the albinism participants are summarized in Supplementary Table 1.

Optical Coherence Tomography

HH-SDOCT (Leica Microsystems, Wetzlar, Germany) was used to obtain a 10 mm x 5 mm high-density volumetric scan (consisting of 100 B-scans and 500 A-scans per B-scan, with a distance of 50 μm between successive B-scans) of the foveal region as previously described.[18] The acquisition speed for each B scan was 5.8 ms with an overall scan time of 2.9 seconds, optical resolution of <4 μm and a digital resolution of 2.4 μm per pixel. This ensured that any motion artifact caused by nystagmus was minimal. Acquisition of an OCT scan was considered successful if the B-scan containing the foveal center was captured together with a minimum of five uninterrupted B scans (i.e., without refixations or blinks on either side of the central foveal B-scan). In all cases, the OCT scan was obtained from the right eye first, followed by the left eye. The acquired images were exported from the OCT software and imported into ImageJ software (available at: http:// rsbweb.nih.gov/ij/; Date accessed: May 11, 2012) where retinal layer segmentation was performed. The lateral scale of each image was estimated using previously reported pediatric axial length data[17] which was also adjusted for refractive error based on information provided by the manufacturer. The nomenclature used to label the segmented layers are based on previously established anatomical correlates with histology.[26,27] One significant difference that should be noted between the anatomical and histological correlates for each retinal layer, is the inclusion of Henle fiber layer as part of the outer nuclear layer on OCT – as this layer cannot normally be visualized on OCT.[27] For the purposes of this study, the parafovea and perifovea were defined as the regions measured at 1000 μm and 2000 μm from the central fovea, respectively.

Statistics and Modelling

Fractional polynomial modelling[28] was used to estimate the mean trajectory (±SEM) of development for each foveal layer thickness with time. Statistical analysis was performed using STATA software (version 14, StataCorp LP, College Station, TX; available at: http://www.stata.com). A polynomial fit was determined for the whole data set (albinism and controls) which was then fitted to each group separately including interaction terms to allow different time courses to be modelled for each group. Applying a single model to the whole data allowed for statistical comparison of differences between the two groups at specific points in time (term, 12 months, 24 months and 60 months post menstrual age (PMA). Results were considered to be significant with a type 1 error rate of less than 0.05 ($p<0.05$).

Results

General Outline of Foveal Morphology and Development in Albinism

We observed a considerable degree of variation in the clinical features and grade of foveal hypoplasia observed in our cohort, suggesting that albinism is a phenotypically highly heterogenous group of conditions (Supplementary Table 1).[29] Interestingly, there was evidence of ongoing foveal development in albinism prior to 40 months postmenstrual age (PMA), with a reduction in foveal IRL thickness and elongation of the outer retinal layers (ORLs) evident in individuals with longitudinal follow-up examinations (Figure 1 & 2).

Total Retinal Thickness

Between birth and 21 months PMA, there was a logarithmic age-related increase in CMT evident from birth, albeit occurring at a reduced rate in albinism in comparison to the control group (Figure 3A). The central macular thickness (CMT) was significantly greater in albinism at all measured time-points in comparison to controls as a result of the presence of significantly thicker inner retinal layers (IRLs) at the fovea (p<0.0001) (Figure 3A, 3B & Supplementary Table 2). In contrast, the parafoveal (1000 μm from the central fovea) and perifoveal (2000μm from the central fovea) retinal thicknesses (RT) were decreased in albinism in comparison to controls (Figure 3A & Supplementary Table 2). This was attributable to significant reductions in the thicknesses of the parafoveal and perifoveal IRLs (Figure 3B & Supplementary Table 2). The degree of foveal excavation (pit depth) was significantly reduced in albinism (21.9 μm, SD 32.1 μm) in comparison to controls (129.4 μm, SD 28.5 μm), p<0.0001. Interestingly, whilst the thickness of the temporal parafoveal and perifoveal outer retinal layers (ORLs) were significantly decreased, the nasal perifoveal ORL thickness was significantly increased in albinism in comparison to controls (Figure 3C & Supplementary Table 2).

Inner Retinal Layers

The IRL thickness was significantly greater in albinism at all measured time-points in comparison to controls at the fovea (p<0.0001) (Figure 3B & Supplementary Table 2). This difference was due to impaired migration of the foveal IRLs, including the retinal nerve fiber (RNFL), ganglion cell complex (GCC) which encompasses the ganglion cell layer (GCL) and the inner plexiform (IPL), and outer plexiform (OPL) in albinism (Figure 4A, 4B, 4C & 4D). Interestingly, there was evidence of ongoing regression of the inner nuclear layer (INL) until approximately 21 months PMA, in both the albinism and control groups. However, in contrast to the control group, the INL never completely regresses from the fovea in the albinism group (Δ=29.0±2.3, p<0.0001 at 69 months PMA). As a result, the mean foveal IRL thickness significantly thicker in albinism (109.1 µm, SD 42.1 µm) in comparison to controls (17.2 µm, SD 18.1 µm) from a combination of significant increases in each of the IRLs. In keeping with impaired IRL migration occurring in the developing albino retina, we found that the parafoveal RNFL was significantly thicker nasally (Δ=2.54±1.3, p<0.0001 at 69 months PMA) and temporally (Δ=3.07±0.87, p<0.0001 at 69 months PMA), whilst the nasal perifoveal RNFL was significantly thinner in albinism (Δ=-5.76±2.3, p<0.0001 at 69 months PMA) (Figure 4A & Supplementary Table 3).

In addition, we observed an altered spatial distribution of each of the inner retinal layers at the parafovea and perifovea. In contrast to the significantly increased central foveal IRL thickness, the parafoveal IRL thicknesses were significantly decreased in albinism as a result of significant reductions in the nasal and temporal GCC thickness, nasal and temporal INL thickness and nasal OPL thickness (Figure 4B, 4C, 4D & Supplementary Table 3).

Outer Retinal Layers

There were significant and interesting differences in the individual ORL thicknesses observed between albinism and control groups. The foveal ORL thickness was significantly decreased in albinism from 21 months of age (Δ=-17.3±4.3, p<0.0001) (Figure 3C & Supplementary Table 2). This was mainly attributable to significantly decreased thicknesses of the foveal photoreceptor inner segments (IS) (Δ=-3.02±1.12, p<0.0001 at 21 months PMA) and photoreceptor outer segments (OS) (Δ=-7.99±1.4, p<0.0001 at 21 months PMA) (Figure 5B, 5C & Supplementary Table 4). Interestingly, there was no significant difference noted in the foveal ONL thickness measurements recorded from the albinism and control groups (Figure 5A & Supplementary Table 4). The perifoveal nasal-temporal ORL thickness asymmetry previously observed appears to be the consequence of a combination of significant increases in the nasal perifoveal outer nuclear layer (ONL) (Δ=10.2±3.17, p<0.0001 at 69 months PMA) and photoreceptor outer segment (OS) (Δ=7.01±0.93, p<0.0001 at 69 months PMA) thicknesses and a significant decrease in the temporal perifoveal ONL (Δ=-4.701±2.7, p=0.004 at 69 months PMA) (Figure 5A, 5C & Supplementary Table 4). In contrast to the foveal OS thickness, which is significantly decreased, the parafoveal OS measurements were significantly increased in albinism in comparison to controls (Figure 5C & Supplementary Table 4). A Pearson's product-moment correlation was run to assess the relationship between foveal OS thickness and foveal excavation in albinism. There was a moderate positive correlation between foveal OS thickness and foveal excavation, r(177) = 0.365, p < .0001. There was a uniform decrease in retinal pigment epithelium (RPE) thickness across all measured retinal locations in albinism (Figure 5D & Supplementary Table 4).

Discussion

Normal retinal development is complex, non-linear, continues until adolescence and involves centrifugal migration of the inner retinal layers (IRLs) away from the foveal centre, centripetal migration of the cone photoreceptors into the foveal centre and elongation of the outer retinal layers (ORLs) over time.[5,30-32] Normally, melanin and L-DOPA determine the differentiation, migration and spatial distribution of the neuronal cells within the mammalian retina.[33,34.] L-DOPA and other tyrosinase dependent signalling molecules have also been shown to have a key role in directing the correct neuronal projections to the optic chiasm.[10,11,13] It has been demonstrated that L-DOPA acts through the OA1 G-protein coupled receptor to upregulate PEDF, a molecule that appears to be crucial for normal retinal development.[35,36] Consistent with disruption of normal retinal development caused by impaired melanin and L-DOPA synthesis in albinism, we observed the presence of foveal hypoplasia on OCT examination in our participants with albinism. This suggests that a deficiency of L-DOPA or one of its metabolic products in albinism results in impaired migration of the IRLs away from the fovea.

Of note, we observed evidence of ongoing regression of the foveal INL after birth in albinism, although this process appears to arrest at approximately 21 months PMA before it can be completed. We also noted an altered spatial distribution of each of the individual retinal layers at the parafovea and perifovea in albinism. This included an interesting pattern of perifoveal nasal-temporal IRL and ORL thickness asymmetry, where the nasal retinal layers were significantly thicker and the temporal retinal layers were significantly thinner in albinism in comparison to controls. This suggests that there is aberrant neuronal migration occurring within the developing albino retina.

An interesting pattern of OS development was also observed in our cohort, where the parafoveal OS measurements were significantly thicker and the foveal OS measurements were

significantly thinner in albinism in comparison to controls. Normal retinal maturation involves centripetal migration of the cone photoreceptors into the central fovea and cone density measurements have been correlated with the thickness of the ONL[30,37] The pattern of OS development observed in this study may reflect impaired centripetal migration of peripheral cone photoreceptors into the central fovea, resulting in a reduced central foveal photoreceptor density and thickening of the parafoveal and perifoveal OS layer. This suggests that melanin and/or L-DOPA are necessary for the correct spatial distribution of the photoreceptors within the retina, in addition to their established role in directing the correct neuronal projections to the optic chiasm.[10,11,13] There is supporting evidence in the literature for this in non-primate mammals, with a positive correlation between demonstrated between levels of ocular melanin and rod numbers in mice and rabbits with albinism.[16,38,39]

It is interesting to compare *in vivo* retinal development in albinism to our previously reported description of *in vivo* retinal development in achromatopsia (ACHM), a condition also associated with abnormal retinal development – but for a different reason (loss of function in cone photoreceptors).[40] Although both conditions are associated with foveal hypoplasia, interestingly, the CMT is significantly increased in albinism and significantly decreased in ACHM.[40] This reflects the different pathology underlying both conditions with a primary abnormality of neuronal migration in albinism and a loss of function of the cGMP-gated channel in the cone photoreceptors with resultant photoreceptor cell death in ACHM.[41] Retinal development in ACHM is further distinguished from retinal development in albinism, by the absence of perifoveal nasal-temporal IRL and ORL thickness asymmetry, presence of significant reductions in the parafoveal and perifoveal IPL and OPL thicknesses, altered developmental trajectories of the ORLs and evidence of RPE degeneration in ACHM.[40] However, in both conditions there is evidence of ongoing retinal development with regression of the IRLs and elongations of the ORLs, suggesting that there is a period of residual plasticity

that could be targeted in conditions associated with abnormalities of retinal development in infancy. In addition, if the longitudinal *in-vivo* OCT appearance of retinal development is altered in a very specific way for each individual retinal condition, OCT could be used as a unique biomarker for each of these conditions and potentially treatments could be customized and timed to the specific developmental abnormalities identified. Further studies of retinal development in other retinal dystrophies and degenerations are needed to confirm if this is the case.

We have demonstrated multiple abnormalities in the development of the human albino retina, which are likely the result of deficiencies of key molecules that are normally produced as part of the melanin/DOPA synthesis pathway. This study has also demonstrated that retinal development is not arrested in albinism, as previously hypothesized.[4] Ongoing regression of the inner retinal layers and elongation of the outer retinal layers in albinism, although delayed and incomplete in comparison to normal controls, suggest that there is a period of residual plasticity where treatments could potentially be targeted. This presents us with several therapeutic possibilities, some of which are already being administered on a trial basis in oculocutaneous albinism. This includes Nitisinone (an inhibitor of 4-hydroxyphenylpyruvate dioxygenase which acts to increase plasma tyrosine levels), gene therapy whereby adeno-associated virus (AAV) vectors mediate tyrosinase gene replacement and DOPA replacement. [19,21,42-44] It remains to be proven if administration of any of these potential treatments in early infancy and childhood, while there is still residual plasticity in the developing albino retina will help to normalize retinal development and optimize visual function. OCT will likely play an important role in monitoring developmental outcomes in any future treatment trials.

Acknowledgements

a. **Funding/Support:** Medical Research Council, London, UK (grant number: MR/J004189/1 and MR/N004566/1), Ulverscroft Foundation, Leicester, UK, The National Eye Research Centre and Nystagmus Network UK. The sponsor or funding organization had no role in the design or conduct of this research. MGT is supported by the NIHR (CL-2017-11-003).

b. **Financial Disclosures:** No financial disclosures

All data supporting this study are openly available from the University of Southampton repository at https://doi.org/10.5258/SOTON/xxxxx

References

1. Apkarian P. A practical approach to albino diagnosis. VEP misrouting across the age span. *Ophthalmic Paediatr Genet*. Jun 1992;13(2):77-88.
2. Sarvananthan N, Surendran M, Roberts EO, et al. The prevalence of nystagmus: the Leicestershire nystagmus survey. Research Support, Non-U.S. Gov't. *Invest Ophthalmol Vis Sci*. Nov 2009;50(11):5201-6. doi:10.1167/iovs.09-3486
3. Wilson HR, Mets MB, Nagy SE, Kressel AB. Albino spatial vision as an instance of arrested visual development. Research Support, U.S. Gov't, P.H.S. *Vision Res*. 1988;28(9):979-90.
4. McAllister JT, Dubis AM, Tait DM, et al. Arrested development: high-resolution imaging of foveal morphology in albinism. Research Support, N.I.H., Extramural
Research Support, Non-U.S. Gov't. *Vision Res*. Apr 7 2010;50(8):810-7. doi:10.1016/j.visres.2010.02.003
5. Lee H, Purohit R, Patel A, et al. In Vivo Foveal Development Using Optical Coherence Tomography. *Invest Ophthalmol Vis Sci*. Jul 1 2015;56(8):4537-45. doi:10.1167/iovs.15-16542
6. Beermann F, Ruppert S, Hummler E, et al. Rescue of the albino phenotype by introduction of a functional tyrosinase gene into mice. Research Support, Non-U.S. Gov't. *Embo J*. Sep 1990;9(9):2819-26.
7. Hearing VJ, Jimenez M. Mammalian tyrosinase--the critical regulatory control point in melanocyte pigmentation. *The International journal of biochemistry*. 1987;19(12):1141-7.
8. Jimenez M, Maloy WL, Hearing VJ. Specific identification of an authentic clone for mammalian tyrosinase. *J Biol Chem*. Feb 25 1989;264(6):3397-403.
9. Ilia M, Jeffery G. Retinal cell addition and rod production depend on early stages of ocular melanin synthesis. *J Comp Neurol*. May 15 2000;420(4):437-44.
10. Rachel RA, Dolen G, Hayes NL, et al. Spatiotemporal features of early neuronogenesis differ in wild-type and albino mouse retina. *J Neurosci*. Jun 1 2002;22(11):4249-63. doi:20026400
11. Ray K, Chaki M, Sengupta M. Tyrosinase and ocular diseases: some novel thoughts on the molecular basis of oculocutaneous albinism type 1. *Prog Retin Eye Res*. Jul 2007;26(4):323-58. doi:10.1016/j.preteyeres.2007.01.001
12. Cronin TH, Hertle RW, Ishikawa H, Schuman JS. Spectral domain optical coherence tomography for detection of foveal morphology in patients with nystagmus. *J Aapos*. Dec 2009;13(6):563-6. doi:10.1016/j.jaapos.2009.09.019
13. Creel D, Hendrickson AE, Leventhal AG. Retinal projections in tyrosinase-negative albino cats. *J Neurosci*. Jul 1982;2(7):907-11.
14. Williams MA, Pinon LG, Linden R, Pinto LH. The pearl mutation accelerates the schedule of natural cell death in the early postnatal retina. *Experimental brain research*. 1990;82(2):393-400.
15. Martinez-Morales JR, Rodrigo I, Bovolenta P. Eye development: a view from the retina pigmented epithelium. *BioEssays : news and reviews in molecular, cellular and developmental biology*. Jul 2004;26(7):766-77. doi:10.1002/bies.20064
16. Donatien P, Jeffery G. Correlation between rod photoreceptor numbers and levels of ocular pigmentation. *Invest Ophthalmol Vis Sci*. Apr 2002;43(4):1198-203.
17. Maldonado RS, Izatt JA, Sarin N, et al. Optimizing hand-held spectral domain optical coherence tomography imaging for neonates, infants, and children. Research Support, N.I.H., Extramural
Research Support, Non-U.S. Gov't. *Invest Ophthalmol Vis Sci*. May 2010;51(5):2678-85. doi:10.1167/iovs.09-4403
18. Lee H, Proudlock F, Gottlob I. Is handheld optical coherence tomography reliable in infants and young children with and without nystagmus? *Invest Ophthalmol Vis Sci*. 2013;54(13):8152-9. doi:10.1167/iovs.13-13230
19. Jeffery G, Schutz G, Montoliu L. Correction of abnormal retinal pathways found with albinism by introduction of a functional tyrosinase gene in transgenic mice. Research Support, Non-U.S. Gov't. *Dev Biol*. Dec 1994;166(2):460-4. doi:10.1006/dbio.1994.1329

20. Ilia M, Jeffery G. Retinal mitosis is regulated by dopa, a melanin precursor that may influence the time at which cells exit the cell cycle: analysis of patterns of cell production in pigmented and albino retinae. *J Comp Neurol*. Mar 15 1999;405(3):394-405.
21. Gargiulo A, Bonetti C, Montefusco S, et al. AAV-mediated tyrosinase gene transfer restores melanogenesis and retinal function in a model of oculo-cutaneous albinism type I (OCA1). Research Support, N.I.H., Extramural
Research Support, Non-U.S. Gov't. *Mol Ther*. Aug 2009;17(8):1347-54. doi:10.1038/mt.2009.112
22. Onojafe IF, Adams DR, Simeonov DR, et al. Nitisinone improves eye and skin pigmentation defects in a mouse model of oculocutaneous albinism. Research Support, N.I.H., Intramural
Research Support, Non-U.S. Gov't. *J Clin Invest*. Oct 2011;121(10):3914-23. doi:10.1172/JCI59372
23. Gregory-Evans CY, Wang X, Wasan KM, Zhao J, Metcalfe AL, Gregory-Evans K. Postnatal manipulation of Pax6 dosage reverses congenital tissue malformation defects. *J Clin Invest*. Jan 2014;124(1):111-6. doi:10.1172/JCI70462
24. Wang X, Gregory-Evans CY. Nonsense suppression therapies in ocular genetic diseases. *Cell Mol Life Sci*. May 2015;72(10):1931-8. doi:10.1007/s00018-015-1843-0
25. Kruijt CC, de Wit GC, Bergen AA, Florijn RJ, Schalij-Delfos NE, van Genderen MM. The Phenotypic Spectrum of Albinism. *Ophthalmology*. Dec 2018;125(12):1953-1960. doi:10.1016/j.ophtha.2018.08.003
26. Spaide RF, Curcio CA. Anatomical correlates to the bands seen in the outer retina by optical coherence tomography: literature review and model. Research Support, N.I.H., Extramural
Research Support, Non-U.S. Gov't
Review. *Retina*. Sep 2011;31(8):1609-19. doi:10.1097/IAE.0b013e3182247535
27. Drexler W, Sattmann H, Hermann B, et al. Enhanced visualization of macular pathology with the use of ultrahigh-resolution optical coherence tomography. Case Reports
Research Support, Non-U.S. Gov't
Research Support, U.S. Gov't, P.H.S. *Arch Ophthalmol*. May 2003;121(5):695-706. doi:10.1001/archopht.121.5.695
28. Royston P, Sauerbrei W. A new approach to modelling interactions between treatment and continuous covariates in clinical trials by using fractional polynomials. Research Support, Non-U.S. Gov't. *Statistics in medicine*. Aug 30 2004;23(16):2509-25. doi:10.1002/sim.1815
29. Thomas MG, Kumar A, Mohammad S, et al. Structural grading of foveal hypoplasia using spectral-domain optical coherence tomography a predictor of visual acuity? Research Support, Non-U.S. Gov't. *Ophthalmology*. Aug 2011;118(8):1653-60. doi:10.1016/j.ophtha.2011.01.028
30. Hendrickson AE, Yuodelis C. The morphological development of the human fovea. Research Support, Non-U.S. Gov't
Research Support, U.S. Gov't, P.H.S. *Ophthalmology*. Jun 1984;91(6):603-12.
31. Provis JM, Diaz CM, Dreher B. Ontogeny of the primate fovea: a central issue in retinal development. Review. *Prog Neurobiol*. Apr 1998;54(5):549-80.
32. Provis JM, Hendrickson AE. The foveal avascular region of developing human retina. Research Support, Non-U.S. Gov't. *Arch Ophthalmol*. Apr 2008;126(4):507-11. doi:10.1001/archopht.126.4.507
33. Stone J, Rowe MH, Campion JE. Retinal abnormalities in the Siamese cat. *J Comp Neurol*. Aug 15 1978;180(4):773-82. doi:10.1002/cne.901800408
34. Choudhury BP. Ganglion cell distribution in the albino rabbit's retina. *Experimental neurology*. Jun 1981;72(3):638-44.
35. Lopez VM, Decatur CL, Stamer WD, Lynch RM, McKay BS. L-DOPA is an endogenous ligand for OA1. *PLoS biology*. Sep 30 2008;6(9):e236. doi:10.1371/journal.pbio.0060236
36. Roffler-Tarlov S, Liu JH, Naumova EN, Bernal-Ayala MM, Mason CA. L-Dopa and the albino riddle: content of L-Dopa in the developing retina of pigmented and albino mice. *PLoS One*. 2013;8(3):e57184. doi:10.1371/journal.pone.0057184

37. Menghini M, Lujan BJ, Zayit-Soudry S, et al. Correlation of outer nuclear layer thickness with cone density values in patients with retinitis pigmentosa and healthy subjects. *Invest Ophthalmol Vis Sci*. Jan 2015;56(1):372-81. doi:10.1167/iovs.14-15521
38. Jeffery G. The albino retina: an abnormality that provides insight into normal retinal development. Review. *Trends Neurosci*. Apr 1997;20(4):165-9.
39. Jeffery G, Brem G, Montoliu L. Correction of retinal abnormalities found in albinism by introduction of a functional tyrosinase gene in transgenic mice and rabbits. *Brain research Developmental brain research*. Mar 17 1997;99(1):95-102.
40. Lee H, Purohit R, Sheth V, et al. Retinal Development in Infants and Young Children with Achromatopsia. *Ophthalmology*. May 9 2015;doi:10.1016/j.ophtha.2015.03.033
41. Michaelides M, Hunt DM, Moore AT. The cone dysfunction syndromes. Review. *Br J Ophthalmol*. Feb 2004;88(2):291-7.
42. Lee H, Scott J, Griffiths H, Self JE, Lotery A. Oral levodopa rescues retinal morphology and visual function in a murine model of human albinism. *Pigment Cell Melanoma Res*. Mar 2019;doi:10.1111/pcmr.12782
43. Onojafe IF, Adams DR, Simeonov DR, et al. Nitisinone improves eye and skin pigmentation defects in a mouse model of oculocutaneous albinism. *J Clin Invest*. Oct 2011;121(10):3914-23. doi:10.1172/JCI59372
44. Summers CG, Connett JE, Holleschau AM, et al. Does levodopa improve vision in albinism? Results of a randomized, controlled clinical trial. *Clin Experiment Ophthalmol*. Nov 2014;42(8):713-21. doi:10.1111/ceo.12325

Figure Legends

Figure 1: Examples of foveal tomograms from 2 participants with albinism and control subjects illustrating the main features of foveal development with postnatal age.

Foveal hypoplasia is evident in all of the tomograms taken from the albinism group (A). In each case, the most central foveal B-scan is shown – although there may be intra-subject differences in both the orientation and scaling of the tomogram, depending on the age and positioning of the participant and the position of the hand-held OCT probe at the time of image acquisition. There is a reduction in the thickness of the IRLs (outlined by the dashed white lines and includes the RNFL, GCL, IPL, INL and OPL) with increasing age. This is in contrast to the control group, where there are no IRLs visible at the fovea after the first few months of life (B). In both the albinism and control groups, there is elongation of the outer retinal layers (ORLs) (indicated by the white double-sided arrows and includes the ONL, IS and OS) with increasing age.

* and Φ indicate tomograms taken from the same patient at different time points

RNFL = retinal nerve fiber layer; GCL = ganglion cell layer; IPL = inner plexiform layer; INL = inner nuclear layer; OPL = outer plexiform layer; ONL = outer nuclear layer; ELM = external limiting membrane; IS = photoreceptor inner segment; ISE = ellipsoid of the inner segment of the photoreceptor; OS = photoreceptor outer segment; RPE = retinal pigment epithelium; IRLs = inner retinal layers; ORLs = outer retinal layers

Figure 2: Developmental trajectories for retinal thickness, inner retinal layers and outer retinal layers at the fovea for participants with albinism with longitudinal measurements.

The plots for each panel show the trajectories plotted over a time period spanning 0 through 100 months postmenstrual age. Each participant has been represented by a different color and each point represents a single value from each OCT examination.

PMA = postmenstrual age

Figure 3: Developmental trajectories for the retinal thickness, inner retinal layers and outer retinal layers at the fovea, parafovea and perifovea.

The plots for each panel show the trajectories plotted over a time period spanning 0 through 100 months postnatal age. Each point represents a single value from each OCT examination. The lines of best fit (trend lines) are shown in blue and red for the albinism and control groups, respectively.

* and ** indicates significance at <0.05 and < 0.01, respectively

PMA = postmenstrual age

Figure 4: Developmental trajectories for the retinal nerve fibre, ganglion cell, inner plexiform, inner nuclear and outer plexiform layers.

The plots for each panel show the trajectories plotted over a time period spanning 0 through 100 months postnatal age. Each point represents a single value from each OCT examination.

The lines of best fit (trend lines) are shown in blue and red for the albinism and control groups, respectively.

* and ** indicates significance at <0.05 and < 0.01, respectively

PMA = postmenstrual age

Figure 5: Developmental trajectories for the outer nuclear, photoreceptor inner segment, photoreceptor outer segment and retinal pigment epithelium layers.

The plots for each panel show the trajectories plotted over a time period spanning 0 through 100 months postnatal age. Each point represents a single value from each OCT examination. The lines of best fit (trend lines) are shown in blue and red for the albinism and control groups, respectively.

* and ** indicates significance at <0.05 and < 0.01, respectively

PMA = postmenstrual age

Figure - label number in Description field; no PDFs

Click here to access/download;Figure - label number in Description field; no PDFs;Figure 1.tif

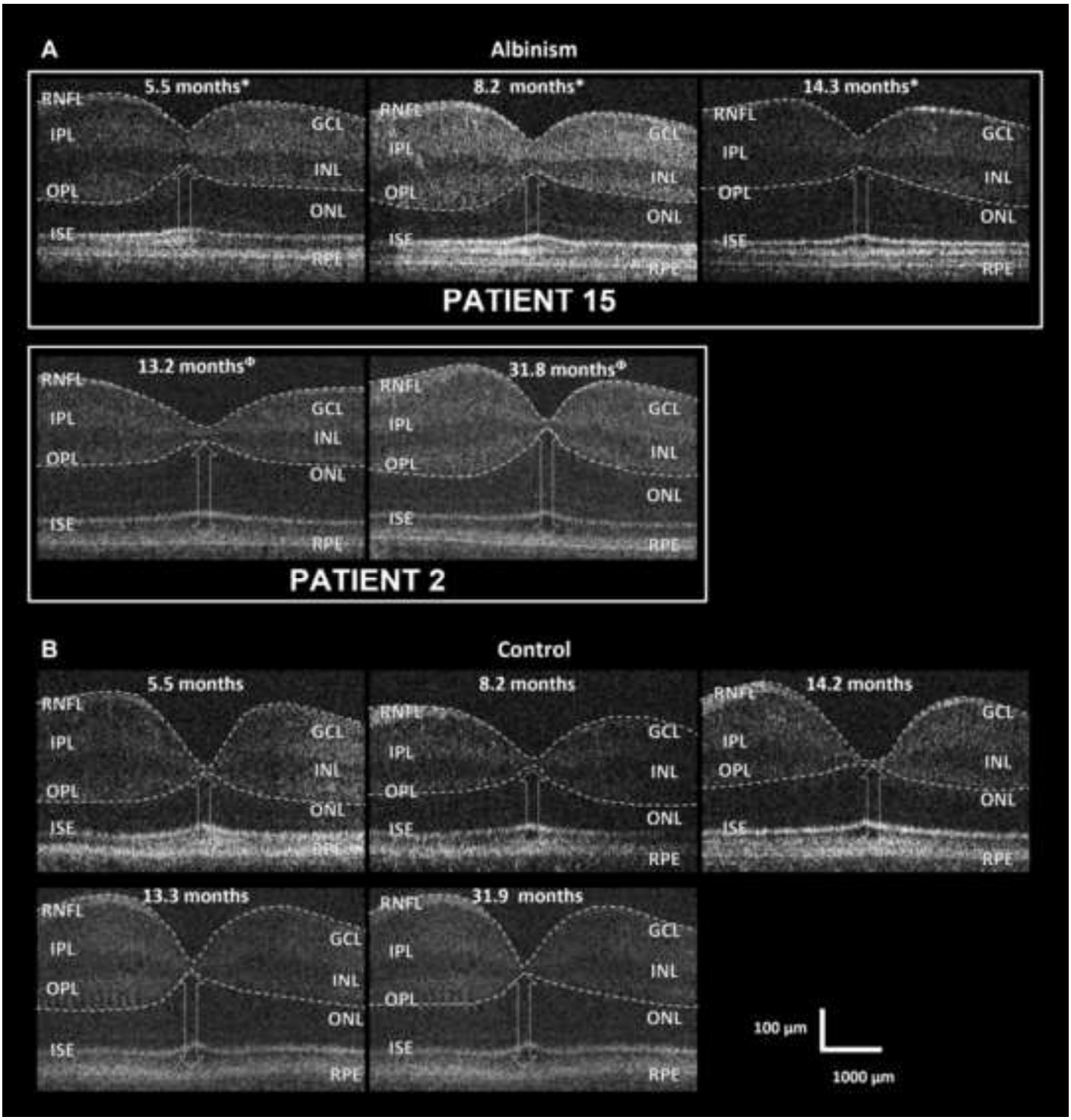

Figure - label number in Description field; no PDFs

Click here to access/download;Figure - label number in Description field; no PDFs;Figure 2.tif

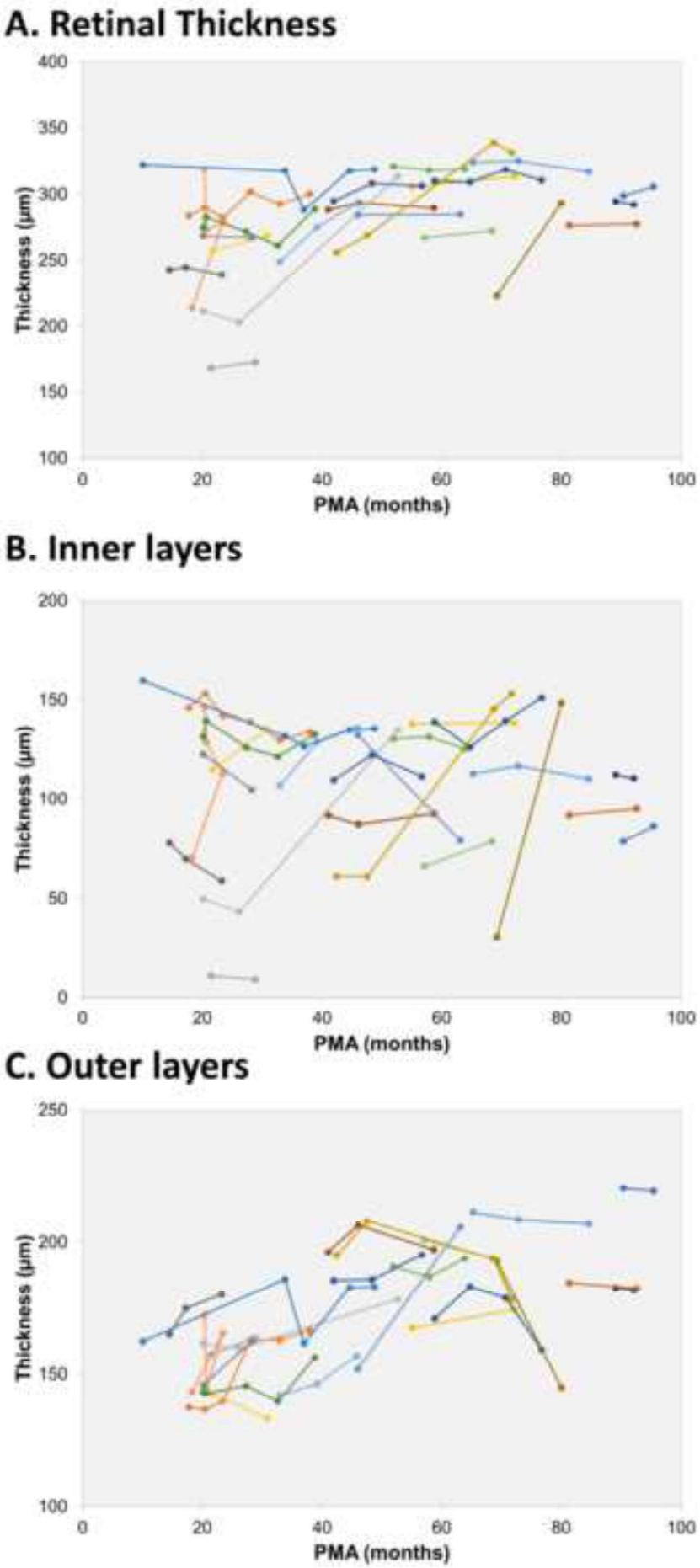

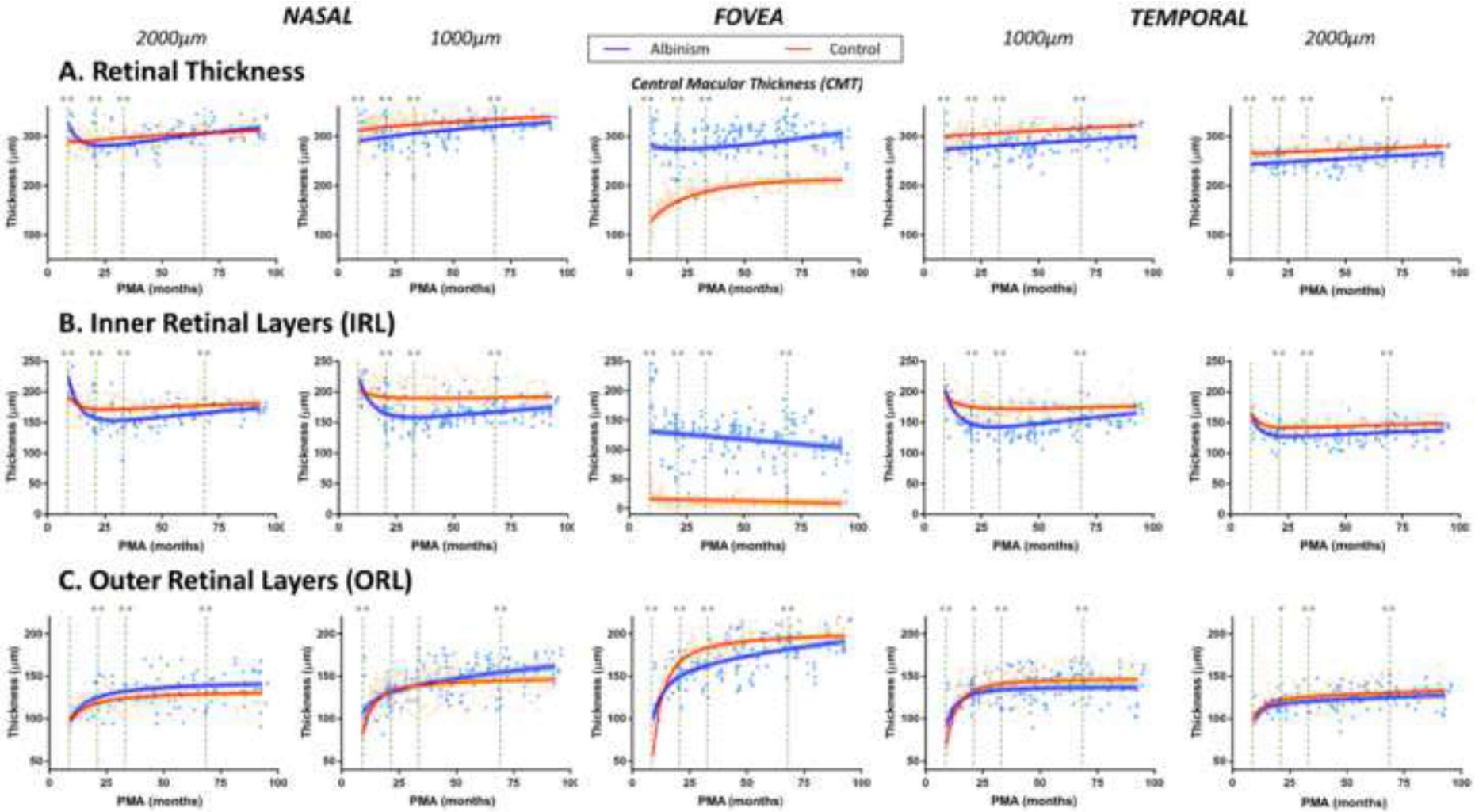

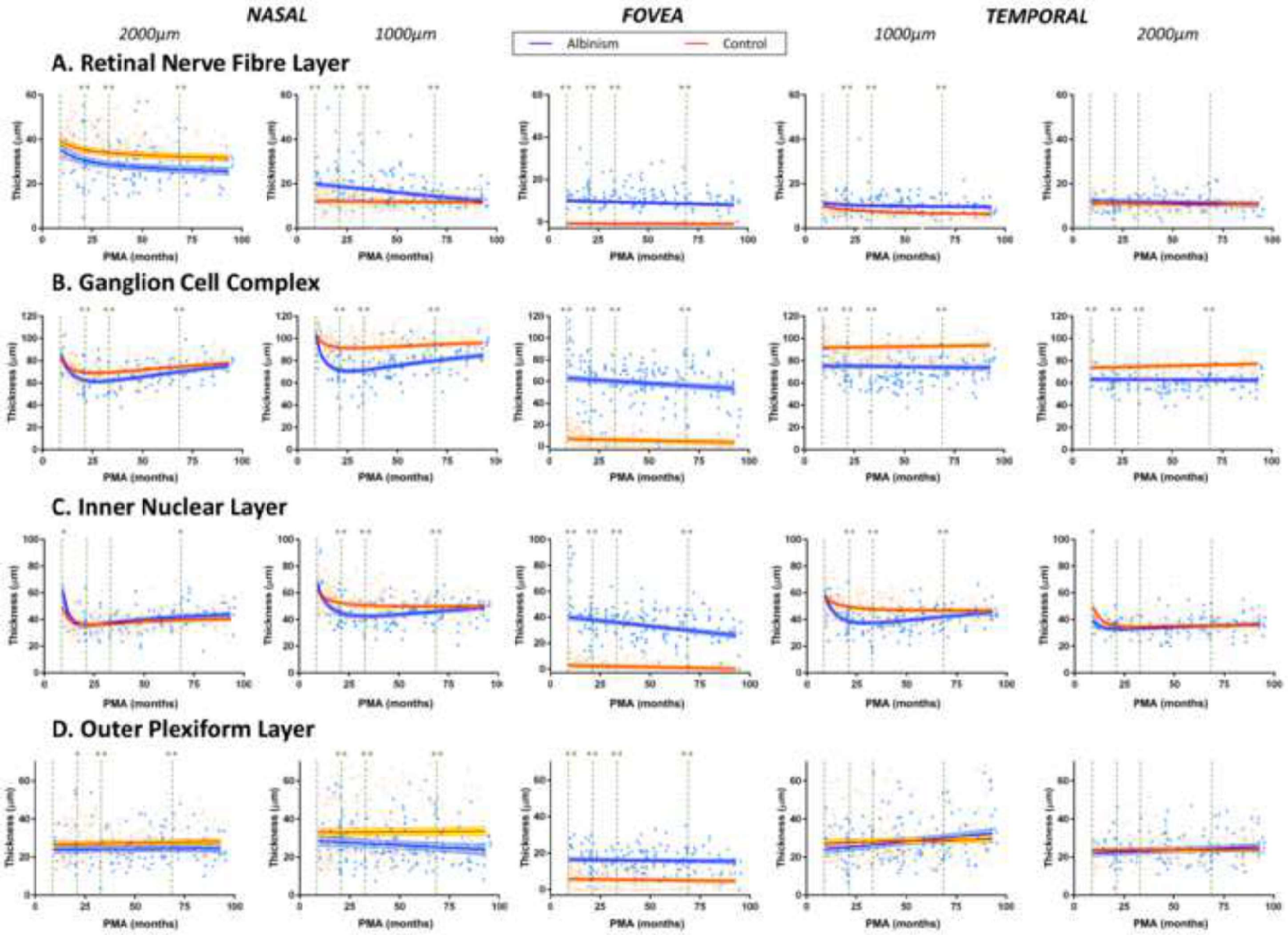

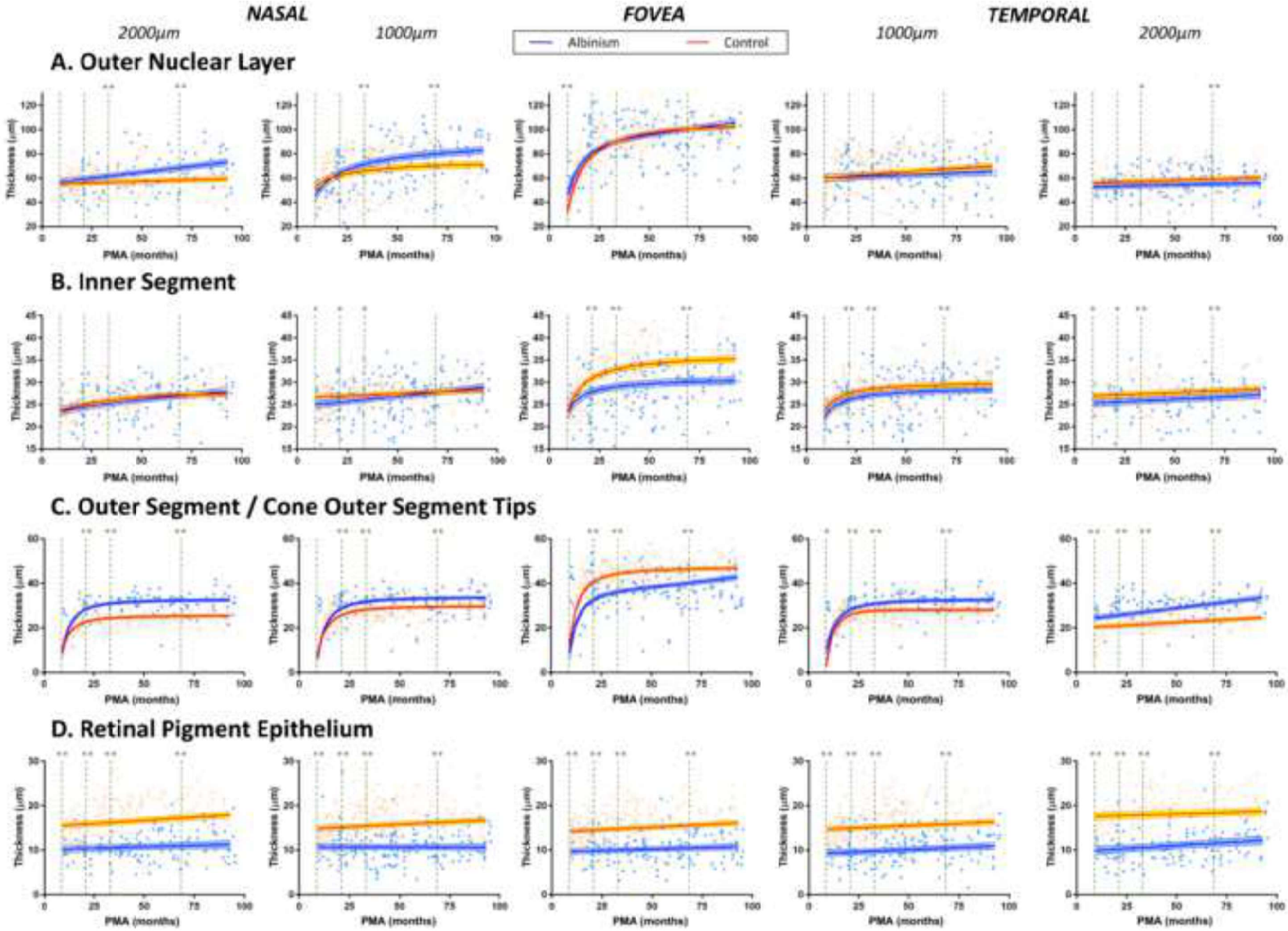

In this prospective, comparative cohort) study of *in vivo* retinal development in 36 children with albinism, evidence of ongoing retinal development in early childhood in albinism has been demonstrated using *in vivo* hand-held optical coherence tomography imaging. Potentially treatment during this critical period may improve retinal development and optimize visual function

Table 1: Clinical Characteristics of Albinism Participants

ID	Sex	Age (months)	VA (LogMAR)†		Refraction		TID	FH Grade*		VEP
			OD	OS	OD	OS		OD	OS	
1	M	29.1	1.20	2.10	+1.20/-1.50@33	+8.50/-1.25@173	Y	2	2	Crossed Asymmetry
2	F	13.2	0.40	0.40	+1.00/-2.50@180	+1.00/-2.50@180	Y	1	1	Normal
		13.3	0.40	0.40	+1.00/-2.50@180	+1.00/-2.50@180		1	1	
		31.8	0.75	0.75	-0.75/-1.25@180	-0.50/-1.00@180		1	1	
		36.4	0.75	0.75	-0.75/-1.25@180	-0.50/-1.00@180		1	1	
3	F	56.2	0.75	0.73	+7.00/-3.00@180	+8.50/-2.50@180	Y	1	1	Crossed Asymmetry
		63.8	0.65	0.65	+7.25/-2.50@180	+8.25/-2.00@180		1	1	
		75.6	0.85	0.78	+7.00/-2.00@180	+8.00/-1.75@180		1	1	
4	M	50.5	0.60	0.45	-2.50/-2.25@180	-2.50/-2.25@180	Y	1	1	Normal
		53.5	0.40	0.35	-2.50/-2.25@180	-2.50/-2.25@180		1	1	
		63.2	0.55	0.55	-2.75/-2.50@5	-2.25/-1.75@175		1	1	
		69.2	0.53	0.43	-2.00/+2.76@180	-2.00/+1.50@180		1	1	
5	F	15.9	0.60	0.60	+1.00/-1.00@10	+1.00/-1.25@170	Y	1	1	Normal
		26.2	---	---	+1.25/-1.00@5	+1.75/-1.50@170		1	1	
6	F	8.7	0.80	0.80	+0.25/+0.50@90	+0.25/+0.50@90	Y	3	3	Crossed Asymmetry
		11.4	1.00	1.00	+0.25	+0.25		3	3	
		14.4	0.70	0.70	+0.25/+0.50@90	+0.25		3	3	
		19	---	---	+4.00	+4.00		3	3	
		23.9	---	---	+4.00	+4.00		3	3	
		28.93	0.80	0.80	+4.50	+4.50		3	3	
7	M	4.5	1.60	1.60	---	---	Y	0	0	Crossed Asymmetry
		12.4	0.90	0.90	---	---		0	0	
		19.8	1.00	1.00	---	---		0	0	
8	M	46.1	0.50	0.60	+0.75/+0.75@170	+0.75/+0.75@75	Y	3	3	Normal
		63.1	0.83	0.80	+1.75/-0.50@10	+1.75/-0.50@170		3	3	
9	M	42.9	1.00	0.95	+0.00/-3.25@16	+0.25/-2.75@167	Y	2	2	---
		48.9	0.90	1.00	+0.00/-3.25@16	+0.00/-2.75@167		2	2	
		54.9	0.75	0.75	+0.00/-3.25@16	+0.00/-2.75@167		2	2	
10	F	45	0.85	0.75	+4.00	+4.00	Y	1	1	Normal
		47.5	0.70	0.75	+6.00/-0.50@155	+5.50		1	1	
		62.2	0.65	0.60	+6.50/-0.75@150	+5.75		1	1	
11	M	52.27	0.50	0.50	+0.00/+1.00@90	+0.00/+1.00@90	Y	1	1	Normal
12	M	49.8	1.00	1.00	+5.50/-3.00@5	+6.50/-3.50@100	Y	3	3	Crossed Asymmetry
		55.7	1.00	1.00	+5.50/-3.00@5	+6.50/-3.50@180		3	3	
		61.7	1.00	1.00	+6.00/-3.50@5	+6.00/-3.50@175		3	3	
		67.7	1.00	1.00	+6.00/-3.50@5	+6.00/-3.50@175		3	3	
13	M	26.8	0.90	0.90	---	---	Y	1	1	Crossed Asymmetry
14	M	32	0.60	0.50	+3.00/+1.00@90	+3.00/+1.00@90	Y	1	1	Crossed Asymmetry
		37.1	0.80	0.70	+3.00/+1.00@90	+3.00/+1.00@90		1	1	
		49.7	0.70	0.65	+5.75/-1.75@51	+4.50/-1.25@177		1	1	
15	M	5.5	---	---	+2.00/+0.50@90	+2.00/+0.50@90	Y	1	1	

		8.2	1.00	1.00	+2.00/+0.50@90	+2.00/+0.50@90		1	1	Crossed Asymmetry
		14.2			+2.00/+0.50@90	+2.00/+0.50@90		1	1	
16	M	57.8	0.70	0.70	---	---	Y	3	3	Crossed Asymmetry
17	M	0.92	---	---	+1.50	+1.50	Y	4	4	Crossed Asymmetry
		1.1	---	---	+1.50	+1.50		4	4	
		1.6	---	---	+1.50	+1.50		4	4	
		2	---	---	+1.50	+1.50		4	4	
		10.5	1.00	1.00	+0.50	+0.50		4	4	
18	F	11.6	---	---	---	---	Y	3	3	Crossed Asymmetry
		14.4	1.00	1.00	---	---		3	3	
19	M	14.7	0.50	0.50	---	---	Y	1	1	Unreliable
		21.4	---	---	---	---		1	1	
		31.4	---	---	---	---		1	1	
		37.7	0.50	0.50	---	---		1	1	
20	M	9.2	0.70	0.70	+3.00	+3.00	Y	1	1	Crossed Asymmetry
		11.1	0.90	0.90	+3.00	+3.00		1	1	
		17.1	0.60	0.60	+3.00	+3.00		1	1	
21	M	12.7	---	---	+6.50/+1.00@90	+6.50/+1.00@90	Y	4	4	Crossed Asymmetry
		21.9	0.70	0.70	+7.50/-0.50@180	+7.00		4	4	
22	M	54.1	0.50	0.33	+5.50	+6.00	Y	1	1	Normal
23	M	10.2	1.00	1.00	---	---	N	3	3	Crossed Asymmetry
24	M	71	0.28	0.20	+3.50/-2.00@25	+4.50/-2.00@10	Y	3	3	Crossed Asymmetry
25	M	80.1	0.55	0.55	+1.00/+1.50@100	+0.25/+2.75@85	Y	1	1	Crossed Asymmetry
		83.1	0.53	0.58	+1.00/+1.50@100	+0.25/+2.75@85		1	1	
26	M	54.5	0.40	1.75	+4.50/-1.50@20	+6.00/-2.00@160	Y	1	1	Crossed Asymmetry
		75.8	0.63	0.63	+4.50/-1.50@20	+6.00/-2.00@160		1	1	
27	M	23.9	---	---	+3.00/-4.00@15	+3.50/-4.00@162	Y	4	4	Unreliable
		30.2	---	---	+3.00/-4.00@15	+3.50/-4.00@162		4	4	
		36.8	0.95	1.05	+2.50/-3.40@30	+3.00/-3.50@160		4	4	
28	F	11.3	---	---	+7.00	+7.00	Y	1	1	---
29	M	48.1	0.85	0.80	-0.50/+0.75@180	_0.50/+1.00@180	N	1	1	Crossed Asymmetry
		59.4	0.65	0.75	_0.50/+1.00@130	-1.50/+0.75@110		1	1	
30	F	43.6	0.70	0.80	+4.00/-3.00@180	+4.50/-3.00@180	Y	2	2	Crossed Asymmetry
31	M	37	1.30	1.30	---	---	Y	4	4	Unreliable
32	F	37.9	1.20	1.20	+2.50/-4.25@179	+3.00/-4.25@2	Y	4	4	---
33	F	6.6	1.30	1.30	+1.50/+1.50@90	+1.50/+1.50@90	Y	4	4	Crossed Asymmetry
34	M	16.2	1.60	1.60	-0.50/0.5@180	-0.50/0.50@180	N	1	1	Crossed Asymmetry
		24.5	0.60	0.60	-0.50/0.5@180	-0.50/0.50@180		1	1	
35	M	58.55	0.30		+2.00/+1.75@90		Y	1		Increased Latency
		61.51	0.60		+2.00/+1.75@90			1		
		73.28		0.53		+2.00/+1.75@90			1	
36	M	24.8	0.90	1.00	+4.00/-6.00@180	+4.00/-6.00@180	Y	4	4	Crossed Asymmetry
		28	1.50	1.50	+4.00/-6.00@180	+4.00/-6.00@180		4	4	

		35.6 39.7	1.10 1.20	1.00 1.20	+2.50/-6.00@5 +3.00/-6.00@180	+4.00/-6.00@180 +4.00/-6.00@180		4 4	4 4	
37	F	72.3 83.6	0.40 0.50	0.45 0.50	+2.25 +2.25	+2.50/-0.75@100 +2.75/-0.25@45	Y	1 1	1 1	Crossed Asymmetry
38	M	36.3	0.70	0.70	+4.25/+1.50@85	+5.00/+1.00@90	Y	4	4	Crossed Asymmetry
39	F	4.64 7.63 16.87	1.50	1.50 --- 0.70	+0.25/-1.0@180	+0.25/-1.0@180 +0.25/-1.0@180 +0.25/-1.0@180	Y	1	1 1 1	---
40	F	83.4	0.60	0.60	+5.50/-2.50@170	+5.25/-2.50@10	Y	1	1	Crossed Asymmetry
41	M	66.5 76.9	0.60 0.65	0.68 0.50	+3.75/-1.00@4 +3.50/-1.00@175	+4.00/-1.00@178 +4.00/-1.00@175	Y	1 1	1 1	Unreliable
42	M	33.4 38.5 47.3	0.90 --- 0.35	--- 0.50 0.45	+1.5 +1.5 +1.5	+1.5 +1.5 +1.5	Y	1 1 1	1 1 1	Normal
43	M	59.7 62.7	0.45 0.58	0.65 0.70	+5.00/-3.00@2 +5.00/-3.00@2	+5.50/-2.50@5 +5.50/-2.50@5	Y	2 2	2 2	Crossed Asymmetry

Albinism was diagnosed based on the presence of at least two positive signs from: (1) iris transilllumination defects, (2) presence of foveal hypoplasia on optical coherence tomography (OCT) examination and (3) the presence of crossed asymmetry on visual evoked potentials.

† In some cases, the BCVA appeared to decrease with age. This can be attributed to a change in the type of visual acuity testing being performed (e.g. from Teller acuity cards in younger infants to Glasgow acuity cards in older children) in addition to variable levels of cooperation with visual acuity testing at different ages.

* Foveal hypoplasia was graded based on the classification system described by Thomas et al[28] as follows: Grade 1 = shallow foveal pit, Grade 2 = absent foveal pit but photoreceptor outer segments (OS) lengthening and outer nuclear layer (ONL) widening present, Grade 3 = Grade 2 foveal hypoplasia with absence of OS lengthening and Grade 4 = Grade 3 with absence of ONL widening. A grade of zero indicates no evidence of foveal hypoplasia on OCT examination.

ID = identification number; M = male; F = female; BCVA = best-corrected visual acuity; RE = right eye; LE = left eye; VEP = visual evoked potential; TID = iris transilllumination defects; Y = yes; N = no; FH = foveal hypoplasia; VEP = visual evoked potentials, OS = photoreceptor outer segments, ONL = outer nuclear layer

A. Retinal Thickness

	2000 µm nasal				1000 µm nasal				fovea				1000 µm temporal				2000 µm temporal			
age	Δ	LCI	UCI	*P*	Δ	LCI	UCI	*P*	Δ	LCI	UCI	*P*	Δ	LCI	UCI	*P*	Δ	LCI	UCI	*P*
9	34.7	16.0	53.4	**0.000**	-22.2	-29.1	-15.3	**0.000**	152.9	137.2	168.6	**0.000**	-26.2	-32.4	-20.0	**0.000**	-21.6	-28.0	-15.1	**0.000**
21	-9.83	-15.6	-4.08	**0.001**	-19.8	-24.5	-15.0	**0.000**	105.8	99.6	112.1	**0.000**	-25.8	-30.8	-20.8	**0.000**	-20.6	-25.9	-15.4	**0.000**
33	-12.7	-17.9	-7.47	**0.000**	-18.0	-21.6	-14.4	**0.000**	88.7	82.7	94.6	**0.000**	-25.5	-29.5	-21.4	**0.000**	-19.7	-23.9	-15.4	**0.000**
69	-1.13	-5.89	3.63	0.641	-14.0	-18.5	-9.63	**0.000**	83.8	77.7	90.0	**0.000**	-24.4	-28.8	-19.9	**0.000**	-16.8	-20.8	-12.8	**0.000**

B. Inner Retinal Layers

	2000 µm nasal				1000 µm nasal				fovea				1000 µm temporal				2000 µm temporal			
age	Δ	LCI	UCI	*P*	Δ	LCI	UCI	*P*	Δ	LCI	UCI	*P*	Δ	LCI	UCI	*P*	Δ	LCI	UCI	*P*
9	32.0	13.9	50.2	**0.001**	16.2	-0.8	33.2	0.062	115.0	106.5	123.4	**0.000**	9.62	-6.18	25.4	0.233	-4.3	-22.9	14.3	0.650
21	-15.2	-20.6	-9.74	**0.000**	-27.2	-32.9	-21.4	**0.000**	112.0	105.3	118.8	**0.000**	-28.0	-33.3	-22.8	**0.000**	-14.2	-19.3	-9.13	**0.000**
33	-18.7	-23.4	-14.1	**0.000**	-31.3	-36.5	-26.1	**0.000**	109.1	103.6	114.6	**0.000**	-29.7	-34.5	-25.0	**0.000**	-14.2	-18.3	-10.0	**0.000**
69	-12.2	-16.5	-7.87	**0.000**	-23.1	-28.0	-18.1	**0.000**	100.4	94.17	106.6	**0.000**	-18.4	-22.8	-14.0	**0.000**	-12.1	-15.5	-8.62	**0.000**

C. Outer Retinal Layers

	2000 µm nasal				1000 µm nasal				fovea				1000 µm temporal				2000 µm temporal			
age	Δ	LCI	UCI	*P*	Δ	LCI	UCI	*P*	Δ	LCI	UCI	*P*	Δ	LCI	UCI	*P*	Δ	LCI	UCI	*P*
9	0.94	-9.85	11.7	0.864	23.9	6.51	41.2	**0.007**	43.7	28.8	58.7	**0.000**	22.9	8.02	37.8	**0.003**	-0.34	-16.0	15.3	0.966
21	6.76	3.17	10.4	**0.000**	-0.83	-5.93	4.26	0.748	-17.3	-21.6	-13.0	**0.000**	-3.60	-6.85	-0.36	**0.030**	-5.06	-8.98	-1.13	**0.011**
33	8.35	5.59	11.1	**0.000**	0.24	-4.28	4.76	0.917	-20.8	-24.6	-16.9	**0.000**	-7.15	-10.3	-4.02	**0.000**	-5.58	-9.24	-1.93	**0.003**
69	9.80	6.43	13.2	**0.000**	9.80	5.47	14.12	**0.000**	-12.9	-16.6	-9.13	**0.000**	-9.02	-12.5	-5.55	**0.000**	-5.56	-8.55	-2.57	**0.000**

A. Retinal Nerve Fibre Layer

	2000 µm nasal				1000 µm nasal				fovea				1000 µm temporal				2000 µm temporal			
age	Δ	LCI	UCI	*P*	Δ	LCI	UCI	*P*	Δ	LCI	UCI	*P*	Δ	LCI	UCI	*P*	Δ	LCI	UCI	*P*
9	-3.72	-9.81	2.37	0.231	7.72	6.00	9.44	**0.000**	10.9	9.67	12.1	**0.000**	1.27	-0.81	3.34	0.232	1.16	-0.78	3.10	0.241
21	-4.83	-7.45	-2.20	**0.000**	6.68	5.31	8.06	**0.000**	10.6	9.64	11.6	**0.000**	2.24	1.33	3.15	**0.000**	1.00	-0.57	2.57	0.212
33	-5.25	-7.10	-3.40	**0.000**	5.65	4.53	6.76	**0.000**	10.3	9.55	11.1	**0.000**	2.61	1.93	3.30	**0.000**	0.84	-0.44	2.12	0.196
69	-5.76	-8.06	-3.47	**0.000**	2.54	1.26	3.82	**0.000**	9.53	8.62	10.4	**0.000**	3.07	2.20	3.94	**0.000**	0.37	-0.97	1.70	0.591

B. Ganglion Cell Complex

	2000 µm nasal				1000 µm nasal				fovea				1000 µm temporal				2000 µm temporal			
age	Δ	LCI	UCI	*P*	Δ	LCI	UCI	*P*	Δ	LCI	UCI	*P*	Δ	LCI	UCI	*P*	Δ	LCI	UCI	*P*
9	3.07	-6.55	12.68	0.532	-1.52	-11.3	8.29	0.761	55.9	51.5	60.4	**0.000**	-16.3	-19.9	-12.7	**0.000**	-10.4	-13.7	-7.16	**0.000**
21	-7.05	-10.0	-4.08	**0.000**	-20.2	-23.5	-17.0	**0.000**	55.0	51.4	58.6	**0.000**	-16.8	-19.7	-14.0	**0.000**	-11.0	-13.7	-8.37	**0.000**
33	-7.53	-10.2	-4.85	**0.000**	-20.0	-22.8	-17.3	**0.000**	54.1	51.2	57.0	**0.000**	-17.4	-19.7	-15.1	**0.000**	-11.7	-13.8	-9.49	**0.000**
69	-4.54	-6.98	-2.10	**0.000**	-14.4	-17.1	-11.7	**0.000**	51.4	48.10	54.7	**0.000**	-19.0	-21.6	-16.5	**0.000**	-13.5	-15.5	-11.5	**0.000**

C. Inner Nuclear Layer

	2000 µm nasal				1000 µm nasal				fovea				1000 µm temporal				2000 µm temporal			
age	Δ	LCI	UCI	*P*	Δ	LCI	UCI	*P*	Δ	LCI	UCI	*P*	Δ	LCI	UCI	*P*	Δ	LCI	UCI	*P*
9	12.4	0.70	24.1	**0.038**	5.66	-2.21	13.5	0.159	37.1	33.9	40.3	**0.000**	1.34	-6.30	8.97	0.732	-10.6	-20.1	-1.01	**0.030**
21	-0.18	-3.38	3.01	0.910	-7.54	-10.2	-4.87	**0.000**	35.5	32.9	38.0	**0.000**	-10.7	-13.3	-8.20	**0.000**	-2.43	-5.04	0.19	0.069
33	0.42	-1.81	2.66	0.710	-8.05	-10.5	-5.62	**0.000**	33.9	31.8	35.9	**0.000**	-10.4	-12.7	-8.07	**0.000**	-1.10	-3.24	1.05	0.316
69	2.49	0.18	4.80	**0.035**	-3.87	-6.16	-1.57	**0.001**	29.0	26.7	31.3	**0.000**	-4.62	-6.75	-2.49	**0.000**	-0.04	-1.81	1.73	0.966

D. Outer Plexiform Layer

	2000 µm nasal				1000 µm nasal				fovea				1000 µm temporal				2000 µm temporal			
age	Δ	LCI	UCI	*P*	Δ	LCI	UCI	*P*	Δ	LCI	UCI	*P*	Δ	LCI	UCI	*P*	Δ	LCI	UCI	*P*
9	-2.80	-6.12	0.52	0.098	-4.37	-8.79	0.04	0.052	10.61	8.66	12.56	**0.000**	-3.48	-7.14	0.18	0.062	-1.29	-4.46	1.89	0.426
21	-2.92	-5.59	-0.24	**0.033**	-5.13	-8.68	-1.57	**0.005**	10.65	9.08	12.21	**0.000**	-2.54	-5.50	0.41	0.091	-0.94	-3.53	1.65	0.478
33	-3.03	-5.19	-0.87	**0.006**	-5.88	-8.76	-3.00	**0.000**	10.68	9.41	11.95	**0.000**	-1.61	-4.00	0.78	0.188	-0.59	-2.70	1.52	0.583
69	-3.37	-5.66	-1.09	**0.004**	-8.14	-11.4	-4.92	**0.000**	10.78	9.34	12.21	**0.000**	1.20	-1.41	3.81	0.368	0.46	-1.51	2.42	0.650

A. Outer Nuclear Layer

	2000 µm nasal				1000 µm nasal				fovea				1000 µm temporal				2000 µm temporal			
age	Δ	LCI	UCI	*P*	Δ	LCI	UCI	*P*	Δ	LCI	UCI	*P*	Δ	LCI	UCI	*P*	Δ	LCI	UCI	*P*
9	1.60	-3.08	6.28	0.503	-7.81	-17.6	1.98	0.118	13.4	3.42	23.3	**0.008**	-0.06	-5.31	5.19	0.981	-3.09	-7.46	1.29	0.167
21	3.32	-0.46	7.11	0.085	1.77	-2.53	6.07	0.420	2.65	-0.56	5.86	0.106	-0.72	-4.97	3.53	0.741	-3.27	-6.86	0.31	0.074
33	5.04	1.98	8.10	**0.001**	5.44	2.20	8.69	**0.001**	-0.07	-3.13	3.00	0.967	-1.37	-4.82	2.08	0.437	-3.46	-6.38	-0.53	**0.020**
69	10.2	7.03	13.4	**0.000**	9.91	5.78	14.0	**0.000**	-0.24	-3.47	2.99	0.884	-3.33	-7.04	0.37	0.078	-4.01	-6.71	-1.31	**0.004**

B. Inner Segment

	2000 µm nasal				1000 µm nasal				fovea				1000 µm temporal				2000 µm temporal			
age	Δ	LCI	UCI	*P*	Δ	LCI	UCI	*P*	Δ	LCI	UCI	*P*	Δ	LCI	UCI	*P*	Δ	LCI	UCI	*P*
9	-0.15	-2.40	2.11	0.899	-1.67	-2.96	-0.38	**0.011**	0.21	-3.10	3.53	0.900	-1.51	-4.31	1.28	0.288	-1.61	-3.09	-0.12	**0.034**
21	-0.51	-1.65	0.64	0.387	-1.36	-2.40	-0.32	**0.011**	-3.02	-4.14	-1.90	**0.000**	-1.40	-2.35	-0.46	**0.004**	-1.57	-2.79	-0.35	**0.012**
33	-0.62	-1.57	0.34	0.204	-1.04	-1.89	-0.19	**0.016**	-3.91	-4.82	-2.99	**0.000**	-1.37	-2.13	-0.62	**0.000**	-1.53	-2.53	-0.54	**0.002**
69	-0.19	-1.20	0.83	0.715	-0.09	-1.03	0.85	0.845	-4.71	-5.85	-3.58	**0.000**	-1.35	-2.27	-0.42	**0.004**	-1.42	-2.34	-0.50	**0.002**

C. Outer Segment / Outer Segment Tips

	2000 µm nasal				1000 µm nasal				fovea				1000 µm temporal				2000 µm temporal			
age	Δ	LCI	UCI	*P*	Δ	LCI	UCI	*P*	Δ	LCI	UCI	*P*	Δ	LCI	UCI	*P*	Δ	LCI	UCI	*P*
9	-1.13	-5.88	3.63	0.642	-1.17	-5.28	2.95	0.578	-4.21	-10.37	1.94	0.180	6.87	0.58	13.16	**0.032**	4.04	1.96	6.13	**0.000**
21	5.63	4.69	6.57	**0.000**	3.00	2.14	3.85	**0.000**	-7.99	-9.39	-6.59	**0.000**	2.23	0.73	3.72	**0.003**	4.74	3.04	6.45	**0.000**
33	6.54	5.70	7.37	**0.000**	3.55	2.74	4.37	**0.000**	-8.14	-9.57	-6.72	**0.000**	3.16	2.22	4.10	**0.000**	5.44	4.06	6.83	**0.000**
69	7.01	6.08	7.94	**0.000**	3.85	2.94	4.76	**0.000**	-6.26	-7.60	-4.93	**0.000**	4.25	3.18	5.33	**0.000**	7.55	6.28	8.81	**0.000**

D. Retinal Pigment Epithelium

	2000 µm nasal				1000 µm nasal				fovea				1000 µm temporal				2000 µm temporal			
age	Δ	LCI	UCI	*P*	Δ	LCI	UCI	*P*	Δ	LCI	UCI	*P*	Δ	LCI	UCI	*P*	Δ	LCI	UCI	*P*
9	-5.30	-6.77	-3.82	**0.000**	-4.15	-5.37	-2.92	**0.000**	-4.54	-5.69	-3.39	**0.000**	-5.40	-6.66	-4.14	**0.0000**	-7.70	-9.39	-6.01	**0.000**
21	-5.49	-6.68	-4.30	**0.000**	-4.43	-5.42	-3.44	**0.000**	-4.66	-5.58	-3.74	**0.000**	-5.40	-6.41	-4.38	**0.0000**	-7.52	-8.90	-6.14	**0.000**
33	-5.69	-6.65	-4.73	**0.000**	-4.71	-5.51	-3.91	**0.000**	-4.78	-5.53	-4.03	**0.000**	-5.40	-6.22	-4.57	**0.0000**	-7.34	-8.47	-6.22	**0.000**
69	-6.27	-7.30	-5.24	**0.000**	-5.56	-6.47	-4.64	**0.000**	-5.13	-6.00	-4.27	**0.000**	-5.40	-6.31	-4.48	**0.0000**	-6.81	-7.86	-5.75	**0.000**